Waveform Design and System Verification of Millimeter Wave Radar

Master's thesis in Embedded Electronic System Design

ARVID ZIEMANN

Department of Computer Science and Engineering
CHALMERS UNIVERSITY OF TECHNOLOGY
UNIVERSITY OF GOTHENBURG
Gothenburg, Sweden 2019

Master's thesis 2019

Waveform Design and System Verification of Millimeter Wave Radar

ARVID ZIEMANN

UNIVERSITY OF
GOTHENBURG

CHALMERS
UNIVERSITY OF TECHNOLOGY

Department of Computer Science and Engineering
Chalmers University of Technology
University of Gothenburg
Gothenburg, Sweden 2019

Waveform Design and System Verification of Millimeter Wave Radar
ARVID ZIEMANN

Supervisor: Zhongxia Simon He, Department of Microtechnology and Nanoscience
Examiner: Per Larsson-Edefors, Department of Computer Science and Engineering.

Master's Thesis 2019
Department of Computer Science and Engineering
Chalmers University of Technology and University of Gothenburg
SE-412 96 Gothenburg
Telephone +46 31 772 1000

Typeset in LaTeX
Gothenburg, Sweden 2019

Waveform Design and System Verification of Millimeter Wave Radar
ARVID ZIEMANN
Department of Computer Science and Engineering
Chalmers University of Technology and University of Gothenburg

Abstract

In modern radar applications such as autonomous driving, the range resolution of the radar system is of great importance. The key factors for improving the range resolution involve smart waveform and radar sensing design in addition to the signal bandwidth. Another concept when it comes to waveform design, is the idea of designing radar waveforms that are compatible with communication, which could provide efficient spectrum and hardware usage.

In this thesis, we demonstrate the waveform generation and radar sensing process for a linear frequency modulated (LFM) and orthogonal frequency-division multiplexing (OFDM) based radar waveform compatible with communication. The functionality and radar performance of both the radar systems are evaluated through simulations and real-world measurements at a radio frequency of 80 GHz. It is found that the range resolution of both the LFM and OFDM radar systems is 13.2 cm at 1 GHz bandwidth, when using their conventional radar sensing algorithms. With the intent to improve the range resolution without increasing the bandwidth, a super-resolution algorithm known as multiple signal classification (MUSIC) is implemented for the OFDM radar which is able to improve the range resolution down to 6 cm, with the cost of a higher computational complexity than the conventional OFDM and LFM algorithms.

Keywords: OFDM, LFM, Radar, Communication, Range resolution, Computational complexity

Acknowledgements

I would like to thank my supervisor Zhongxia Simon He for suggesting this thesis topic and for his valuable feedback and assistance with lab measurements.

ARVID ZIEMANN, Gothenburg, June 2019

Contents

List of Abbreviations

ADC Analog-to-digital converter
AWG Arbitrary Waveform Generator
BER Bit-error rate
DAC Digital-to-analog converter
LO Local Oscillator
LFM Linear Frequency Modulation
MUSIC MUltiple SIgnal Classification
FFT Fast Fourier Transform
IFFT Inverse Fast Fourier Transform
MSK Minimum-Shift Keying
SNR Signal-to-noise ratio
OQPSK Offset Quadrature Phase-Shift Keying
OFDM Orthogonal Frequency-Division Multiplexing
QPSK Quadrature Phase-Shift Keying
RF Radio frequency
RadCom Radar-communication

1
Introduction

Despite the fact that radar has been around ever since early 1900s, new challenges and possibilities still emerge for the radar [1]. Radars operating in the millimeter band, often called mmWave radar, are capable of attaining bandwidths up to several gigahertz. A wide bandwidth is crucial for achieving a good range resolution, which is a radar performance metric, referring to the radar's ability to distinguish targets that are close in range [2]. Lower frequency radars fall short in this regard, as they are not capable of achieving a wide bandwidth. Nonetheless, in some applications, a good range resolution is not required. Hence, hardware requirements can be reduced since lower bandwidths are used. However, in modern applications such as autonomous driving, range resolution is of great importance for e.g. distinguishing two closely spaced vehicles. Unfortunately, an increase in bandwidth will put a lot of strain on the ADCs, DACs and the hardware that performs the signal processing. Thus, the designer needs to be aware of these limitations.

Another aspect of modern radar design is the concept of radar-communications (RadCom) waveforms that are capable of performing radar sensing and communication simultaneously. Such an integrated system could provide an efficient shared spectrum in addition to reduced hardware usage. The obvious use of such RadCom systems, would be in autonomous applications with the availability of wireless communication links between vehicles in addition to radar sensing.

1.1 Problem description

A challenging aspect of radar design is to find suitable waveforms that meet the demands of a radar system. The concept of designing a joint radar-communication system with sufficient range resolution can see many usages in modern radar applications, one of them being autonomous driving. The waveform design of such a radar system could be quite complex in regards to satisfying both communication and radar requirements.

A linear frequency modulated (LFM) and an orthogonal frequency division multiplexing (OFDM) based RadCom waveform are proposed in [3] and [4] respectively. In both approaches, the waveform generation is mainly discussed, whereas the range resolution is briefly discussed from mainly a simulation perspective. It would therefore be of interest to thoroughly study the range resolution of these waveforms and compare how they perform in a real environment in comparison to simulations. In

[4] the proposed OFDM waveform was tested in the 24 GHz industrial, scientific and industrial (ISM) band, which is a frequency band ranging from 24-24.25 GHz. High radio frequencies (RF) come with benefits such as an increase in available bandwidth and reduced hardware usage [5]. Thereupon, it would be valuable to study the performance of these waveforms at higher frequencies than the 24 GHz ISM band. Additionally, the proposed LFM and OFDM based waveforms are quite different depending upon how they are generated and how their radar sensing algorithms functions. Hence, a comparison in computational cost would be of great interest.

1.2 Project aim

A LFM and OFDM based radar waveform compatible with communication will be designed and evaluated on a radar system model that will be implemented in MATLAB. The radar performance of the waveforms will be compared to one another by evaluating various metrics such as range resolution and accuracy. Additionally, various signal processing methods with the intent to improve the range resolution of the radar will be evaluated. Particularly, a radar sensing algorithm known as multiple signal classification (MUSIC) [6] will be applied to the OFDM radar with the purpose of improving the range resolution and accuracy.

Furthermore, both the LFM and OFDM radar system will be tested in a real-world environment at a RF of 80 GHz. Real-world factors might affect radar performance in various ways that are not considered from a pure simulation perspective. Hence, new meaningful knowledge can be gained by testing the radar system in a real environment to perceive the real-world limiting factors of a high resolution RadCom system. In particular, the thesis will target the following steps:

- Implement a model of the radar system in MATLAB and simulate OFDM and LFM based waveforms and study their impact on radar system performance such as range resolution and accuracy.
- Test and evaluate the radar system in a real environment using lab equipment at Chalmers, MC2. The designed waveforms will be uploaded to an arbitrary waveform generator (AWG) which periodically outputs the waveform to a E-band transmitter. The reflected signal is mixed down to baseband and is received by a oscilloscope for post processing.
- Compare the LFM and OFDM RadCom systems in terms of computational cost.

1.3 Limitations

Some aspects of radar measurement, in particular measuring moving targets can be quite complicated to achieve, especially in a real-world environment. Additionally, it can complicate the design and even have negative impact on radar performance. Although this might be relevant in some cases it will not be a deciding factor in

order to get the measurement results that this thesis is targeting. Hence, this thesis will only focus on measuring stationary targets.

1.4 Outline

This thesis is organized as follows. In Chapter 2, general radar concepts that are necessary for understanding the content of this thesis are explained, followed by a short introduction to the MSK-LFM and OFDM RadCom waveforms. The following Chapter 3, gives a more detailed description of how the waveforms are generated and how their radar sensing algorithms are implemented. In Chapter 4, simulation and in-lab measurement results are presented and evaluated. Furthermore, the computational cost of the algorithms is discussed. A final conclusion of the thesis is given in Chapter 5.

2
Technical background

This chapter introduces general radar concepts that are necessary for understanding the content of this thesis. Additionally, an overview of the two RadCom waveforms evaluated in this thesis is given. In section 2.1 general radar performance metrics are discussed, followed by an introduction to the MSK-LFM waveform in section 2.2 and OFDM waveform in section 2.3.

2.1 Radar performance metrics

This section explains measurement methods and radar performance metrics used in this thesis.

2.1.1 Radar range profile

The main task of a radar is to detect and determine the range of various objects. Range profiles are a convenient way of visualising radar returns from objects in line-of-sight of the radar. The measured range of a target manifests as a peak in the range profile, this peak has a certain main-lobe width in addition to side-lobes. By reducing the amplitude level of the side-lobes or the width of the main-lobe, the radar performance can be improved [2]. This is generally controlled by the radar sensing algorithms and the bandwidth of the signal. For illustration, a range profile is shown in Fig 2.1 where two objects are detected. This method of visualising information about objects is used throughout this thesis for evaluating radar performance.

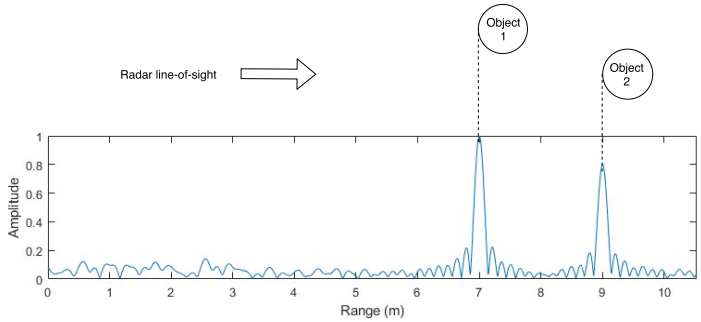

Figure 2.1: Illustration of radar range profile. Two objects are detected and displayed in the range profile.

2.1.2 Range resolution

One common performance metric used for radar is range resolution. This is also known as the radar's ability to detect targets that are close in range. Generally this is measured by examining the -3 dB width of the target main-lobe [2]. Theoretically most radar systems have a range resolution of

$$R = \frac{c_0}{2B} \tag{2.1}$$

where c_0 is the speed of light and B the bandwidth.

By observing (2.1) it is evident that the range resolution can be improved by increasing bandwidth. However, there are other options for improving the range resolution that do not involve increasing the bandwidth. Some of these techniques are based on designing waveforms with good auto-correlation properties [10] or implementing super-resolution algorithms such as the MUSIC algorithm [6, 7].

2.1.3 Accuracy

Accuracy is a radar's ability to measure the true position of an object. The sampling frequency of the radar system is highly correlated to this metric as it more or less determines the time between each sample. Hence, an increase in sampling frequency will diminish the time between each sample which in turn increases the accuracy of the radar.

To explain this concept more thoroughly, consider a radar system sampled at a frequency of 300 MHz. The time between each sample is given by

$$T_s = 1/f_s = \frac{1}{300 * 10^{-6}} = 3.33\,\text{ns} \tag{2.2}$$

corresponding to a distance between each sample, which is given by

$$d_s = c_0 * T_s = c_0 * 3.33 * 10^{-9} = 1\,\text{m} \tag{2.3}$$

hence, there will only be samples at multiples of d_s (0 m, 1 m, 2 m. etc). If a target is located at 2.4 m from the radar, the nearest sampling instance would be at 2 m, thus introducing an error of 0.4 m. By increasing sampling frequency by e.g. two times this error would be reduced, since each sample would be at multiples of 0.5 m, reducing the error to 0.1 m.

Several other factors can impact the accuracy as well. For instance, the side-lobes of close-by targets can influence each other causing a certain offset on the measured target peak.

2.2 The MSK-LFM waveform

This section aims to give an overview of LFM and a method known as MSK used for modulating data. Further on, the concept of combining these waveforms into a radar waveform compatible with communication will be explained.

2.2.1 Linear frequency modulation

The frequency of a LFM waveform, also called “chirp", increases linearly with time. This waveform is commonly used in radar applications because of its good correlation properties used for radar sensing [3]. However, the waveform itself is not able to carry data but because of its good radar properties the most natural approach would be to use it in combination with other waveforms to form a joint radar-communication waveform. The LFM waveform is described in (2.4).

$$s_{LFM}(t) = \cos(2\pi f_c t + \pi \frac{\beta}{T} t^2) - j \sin(2\pi f_c t + \pi \frac{\beta}{T} t^2) \tag{2.4}$$

where f_c is the carrier frequency, β is the frequency sweep range and T the total pulse duration.

2.2.2 Minimum shift keying

Minimum shift keying (MSK) is a digital modulation method that uses two offset transmission frequency slots separated by $\frac{1}{2T}$, T being the bit duration, to transmit data. This is the minimum frequency spacing that still allows sinusoidals to be orthogonal to each other [9]. The data bits are divided into a set of even $a_Q(t)$ and odd $a_I(t)$ bits before they are transmitted over in-phase and quadrature phase carriers. MSK shows similarities to offset quadrature phase shift keying (OQPSK) [9] in the sense that the sign of the transmitted bits cannot change at the same time, hence only allowing phase shifts of ±90 degrees. This is achieved by extending the bit period to $2T$ and skewing the quadrature component by half a bit period T, shown in Fig. 2.2 .

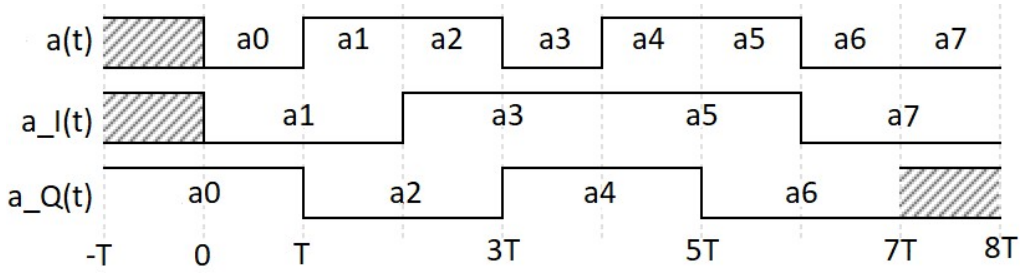

Figure 2.2: Even $a_Q(t)$ and odd $a_I(t)$ bit streams of a MSK signal. The Q-component is skewed by half a bit period T to avoid two bits changing sign simultaneously.

Skewing the quadrature component by half a bit period T eliminates the possibility of ±180 degrees phase shifts, caused by two bits changing sign simultaneously. However, since the bit streams are encoded as square waves they will still cause the signal to make instant 90 degrees phase shifts. This will happen whenever the data bits changes sign, causing phase discontinuities in the signal. This is solved, by encoding each bit of the square wave data streams $a_I(t)$ and $a_Q(t)$ as half sinusoidals.

As a result, the 90 degrees phase shifts will now occur linearly over a time period of T seconds, resulting in a signal with no phase discontinuities. The MSK signal is described by (2.5).

$$s_{MSK}(t) = a_I(t)\cos(\frac{\pi t}{2T})\cos(2\pi f_c t) + a_Q(t)\sin(\frac{\pi t}{2T})\sin(2\pi f_c t) \tag{2.5}$$

where $a_I(t)$ and $a_Q(t)$ are the odd and even bit streams and f_c the carrier frequency. Since the two transmit frequencies of the MSK waveform are located at $f_+ = f_c + \frac{1}{4T}$ and $f_- = f_c - \frac{1}{4T}$ separated by $f_+ - f_- = \frac{1}{2T}$, the carrier frequency needs to be chosen as a multiple of $\frac{1}{4T}$ to ensure a phase continuous signal [9].

A MSK modulator is shown in Fig. 2.3. Initially a bit stream is divided into an even $a_I(t)$ and odd $a_Q(t)$ set of bits with the odd bit stream having a skew of half a bit period shown in Fig. 2.2. The even and odd bit streams are then multiplied with $\cos(\frac{\pi t}{2T})$ and $\sin(\frac{\pi t}{2T})$ respectively to employ the square wave shapes as half sinusoidals. Lastly, the waveforms are modulated on their respective carriers and summed together.

In the demodulator shown in Fig. 2.4, the received signal is multiplied with the in-phase and quadrature phase carriers, followed by a integrator that integrates over a time period of $2T$. Lastly, the output of the integrator is sampled at an interval of $2T$ in order to retrieve the correct bits.

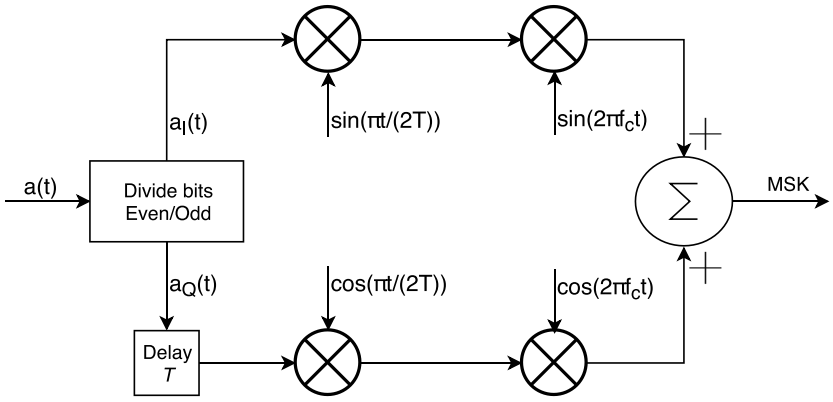

Figure 2.3: MSK modulator.

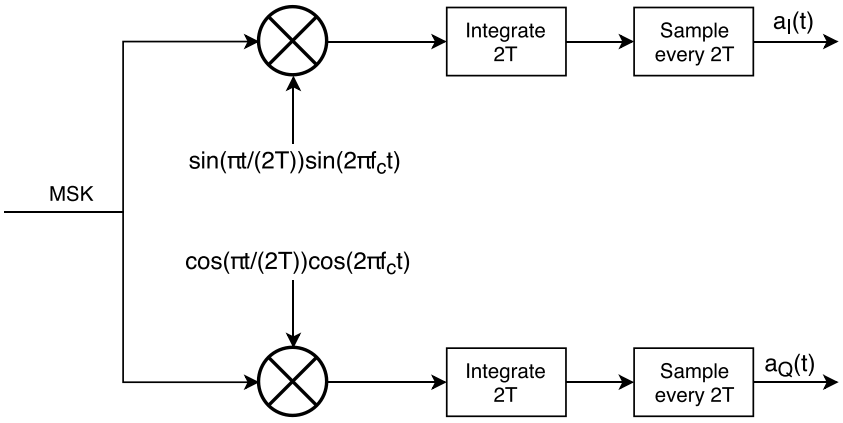

Figure 2.4: MSK demodulator.

2.2.3 Radar-communication waveform composed by MSK and LFM

The MSK-LFM waveform combines the data transmission capabilities MSK provides and the radar sensing attributes of the LFM waveform into a radar-communication waveform capable of both data transmission and radar sensing [3]. The waveform replaces the carrier wave of the MSK waveform with a LFM waveform resulting in a shared and efficient spectrum [11, 12]. Referring to the MSK and LFM waveform the proposed MSK-LFM waveform is given by the following expression:

$$s_{LFM}(t) = \cos(2\pi f_c t + \pi\tfrac{\beta}{T}t^2) - j\sin(2\pi f_c t + \pi\tfrac{\beta}{T}t^2)$$
$$s_{MSK}(t) = a_I(t)\cos(\tfrac{\pi t}{2T})\cos(2\pi f_c t) - a_Q(t)\sin(\tfrac{\pi t}{2T})\sin(2\pi f_c t)$$

$$\boxed{s_{MSK-LFM}(t) = a_I(t)\cos(\frac{\pi t}{2T})\cos(2\pi f_c t + \pi\frac{\beta}{T}t^2) + a_Q(t)\sin(\frac{\pi t}{2T})\sin(2\pi f_c t + \pi\frac{\beta}{T}t^2)} \tag{2.6}$$

By observing the MSK-LFM waveform in (2.6), it can be noted that the baseband signal of the MSK-LFM waveform is the same as that of the MSK signal, thus their properties are the same. The implementation process of the MSK-LFM radar is described more thoroughly in section 3.1.

2.3 The OFDM Waveform

This section will act as an introduction to the most fundamental concepts of the OFDM waveform. Additionally, possibilities for using OFDM for radar sensing are addressed.

2.3.1 Orthogonal subcarriers

Orthogonal frequency-division multiplexing (OFDM) is a widely used data transmission method where the data symbols are transmitted on multiple orthogonal subcarriers (one carrier for each symbol). To maintain orthogonality [16], the frequency spacing between the subcarriers needs to be

$$\Delta f = \frac{1}{T} \tag{2.7}$$

where T is the OFDM symbol duration and Δf the frequency spacing between the subcarriers.

Assuming the subcarrier spacing requirement of Δf is fulfilled, the implementation process of the OFDM transceiver is greatly simplified. The reason for this, is that separate filters for each sub channel are not needed. Instead the orthogonal property of the subcarriers is exploited, which eliminates any possible inter-carrier interference without the need of filters. The OFDM signal is commonly generated by defining the signal in frequency domain with the orthogonal property visualized in Fig. 2.5. The time-domain OFDM signal is then generated using IFFT which can be implemented very efficiently. Generally, the number of subcarriers or choosen as a power of two. This is because the number of subcarriers determines the size of the IFFT operation and it is proven that FFT and IFFT operations that are a power of two can be implemented more efficient [15].

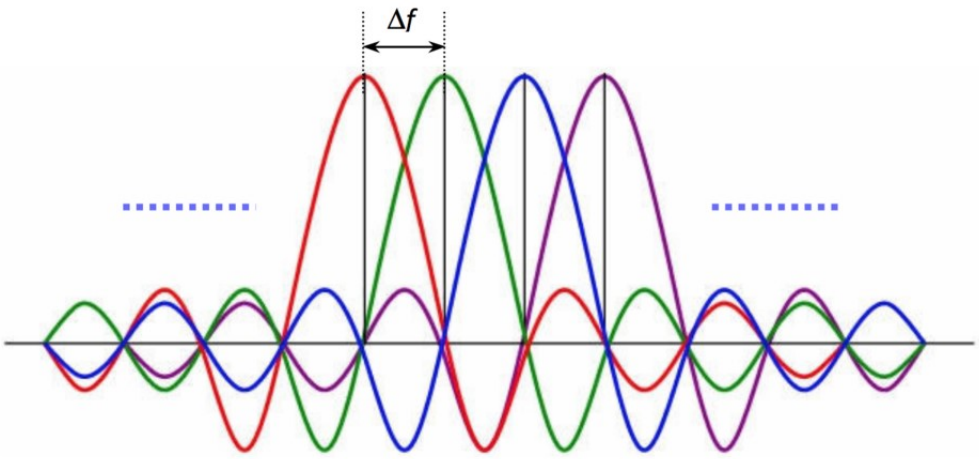

Figure 2.5: OFDM orthogonality property visualized. At each subcarrier's main peak the other subcarriers are at zero amplitude, this property is known as orthogonality and is achieved by having a subcarrier spacing of Δf.

2.3.2 Cyclic prefix

In an ideal transmission channel, the orthogonality between the OFDM subcarriers would be maintained and the FFT operation at the receiver would be able to separate

each subchannel. However, in most cases the transmission channel is distorted in some way, consequently destroying the orthogonality between the subcarriers and introducing interference between adjacent OFDM symbols also known as inter-symbol interference (ISI). This unwanted effect can be mitigated by prepending a cyclic prefix at the beginning of each symbol to act as a guard interval between adjacent OFDM symbols. The cyclic prefix is simply a copy from a part of the end of each OFDM symbol.

2.3.3 Radar sensing possibilities

OFDM signals has the drawback of having imperfect auto-correlation properties [4]. Hence, the classical approach of using cross-correlation for radar sensing has not been successful for OFDM. A more recent technique [4, 13, 14] takes another approach which will be discussed in this thesis. The proposed technique merely operates on the complex OFDM symbols and aims to cover the shortcomings of the OFDM cross-correlation method. Alongside this method, another radar sensing algorithm known as MUSIC will be evaluated and is described in section 3.2.

3

Implementation

In the previous chapter the underlying concepts of the OFDM and MSK-LFM waveform were described. This chapter aims to give more detailed description on how the waveforms are generated and how their corresponding radar sensing algorithms are implemented.

3.1 MSK-LFM radar implementation

In this section, the implementation of the MSK-LFM transmitter is outlined, followed by a description of implementing the receiver and its corresponding radar sensing algorithm.

3.1.1 Transmitter

The implementation process of the MSK-LFM transmitter is similar to the MSK modulator described in the previous chapter. Just as with the MSK modulator, a bit stream $a(t)$ is split into an even and odd set of bits which are then employed as half sinusoidals by multiplying the I and Q signals with $\sin(\frac{\pi t}{2T})$ and $\cos(\frac{\pi t}{2T})$ respectively. The next step differs somewhat from the MSK method, instead of modulating the I and Q signals on a simple carrier wave (as in MSK) they are modulated on a LFM-chirp creating the combined MSK-LFM waveform with a continuous phase and the ability to carry information bits. The block-diagram of the generation process of the MSK-LFM waveform is shown in Fig. 3.1.

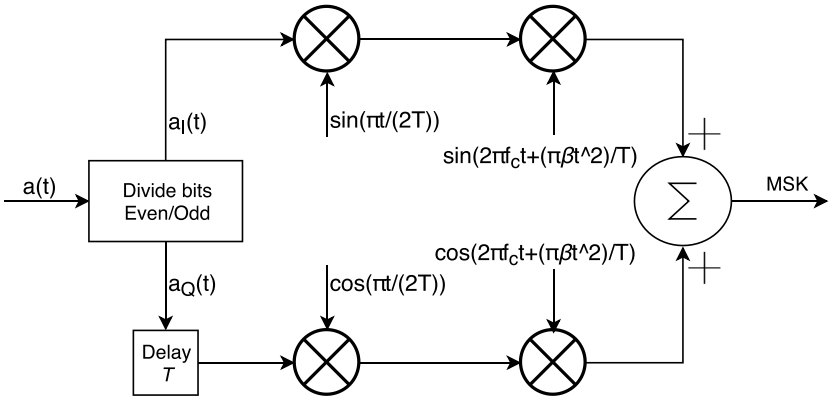

Figure 3.1: MSK-LFM transmitter. A block diagram showing how each step of the transmitter is implemented to generate the MSK-LFM waveform.

3.1.2 Receiver

The MSK-LFM waveform is constructed in such a way that the receiver can use the same waveform to perform radar sensing and demodulation of the communication symbols, namely it does not need to know which waveform is for radar or communication. Hence, the MSK-LFM receiver can be split up into two separate parts that perform demodulation of the communication symbols and radar sensing respectively. The demodulation process for obtaining the communication symbols is very similar to the MSK demodulator described in section 2.2.2 with the exception of the carrier being replaced with an LFM signal.

The radar sensing unit is implemented using a cross-correlation approach, particularly the delay and doppler information can be obtained by (3.1)

$$X(\tau, f_d) = \int_{-\infty}^{\infty} s(t)g^*(t-\tau)e^{j2\pi f_d t}dt \tag{3.1}$$

where $s(t)$ is the transmitted MSK-LFM signal, $g(t)$ the received signal at time lag τ and * the complex conjugate.

Since we are mainly interested in measuring stationary targets the doppler-shift f_d can be set to zero. As a result, (3.1) simplifies to

$$X(\tau, 0) = \int_{-\infty}^{\infty} s(t)g^*(t-\tau)dt \tag{3.2}$$

we note that (3.2) is the cross-correlation between $s(t)$ and $g(t)$. In other terms, it can be referred to as taking the convolution of the transmitted $s(t)$ and received $g(t)$ signal with the complex conjugate and time-reversal being computed on either the transmitted or received signal. This operation can be implemented in various ways, the more efficient way is to compute the correlation operation in the frequency domain instead of the time domain, known as fast convolution, shown in Fig. 3.2. This operation requires an FFT and IFFT unit in addition to a multiplier. Note, that only the FFT of the received signal needs to be computed as the FFT of the transmitted reference signal can be stored in memory.

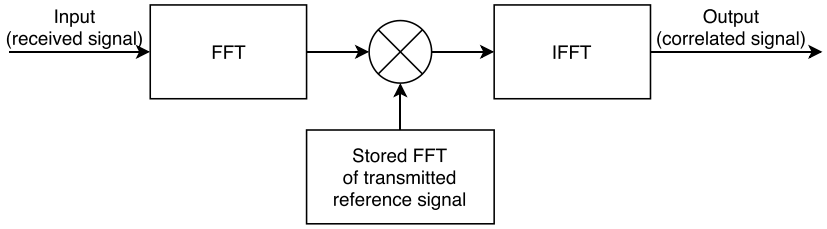

Figure 3.2: Frequency domain correlation used by the MSK-LFM radar for radar sensing.

3.2 OFDM radar implementation

The implementation process of the OFDM transmitter and receiver is described in this section. A radar sensing algorithm merely operating on the OFDM symbols is outlined in addition to a super-resolution algorithm known as MUSIC.

3.2.1 Transmitter

The block diagram of the OFDM transmitter is shown in Fig. 3.3. Initially, a set of data bits are encoded to QPSK symbols. These symbols are then passed through a serial to parallel converter. The symbol frames can then be regarded as a matrix S shown in (3.3) where each row represents one subcarrier and each column one OFDM symbol.

$$S = \begin{bmatrix} s(0) & s(N_{sub}) & \dots & s((N_{sym}-1)N_{sub}) \\ s(1) & s(N_{sub}+1) & \dots & s((N_{sym}-1)N_{sub}+1) \\ \cdot & \cdot & \dots & \cdot \\ \cdot & \cdot & \dots & \cdot \\ \cdot & \cdot & \dots & \cdot \\ s(N_{sub}-1) & s(2N_{sub}-1) & \dots & s(N_{sym}N_{sub}-1) \end{bmatrix} \tag{3.3}$$

The IFFT is then computed on each OFDM symbol corresponding to each column of matrix S, creating a time domain OFDM signal. To eliminate possible intersymbol interference, a guard-interval is inserted between the OFDM symbols by adding a cyclic-prefix at the start of each symbol, consisting of a part of the end of the symbol. After cyclic-prefix insertion, the matrix representation of the signal is converted back to a serial representation. The signal is then interpolated and modulated on a given carrier frequency.

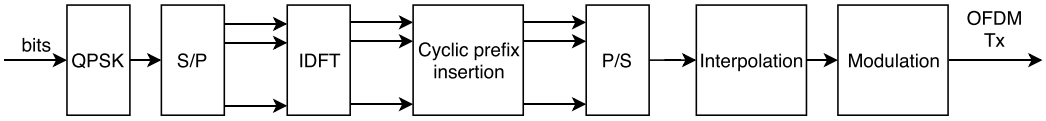

Figure 3.3: OFDM transmitter.

3.2.2 Receiver

Excluding synchronization and equalization, the reverse effect of the transmitter side is computed on the receiver side shown in Fig. 3.4. Particularly, the received signal is demodulated to baseband and decimated. The resulting signal is converted to a matrix representation. The cyclic prefix is then removed followed by a FFT operation on each column of the matrix. At this stage, the channel in which the OFDM signal is sent over might alter the information of the OFDM symbols. The effect of this channel needs to be removed or at the very least reduced. One way to do so is called equalization, in which the channel is estimated by dividing a part of the received and transmitted symbols. Hence, a certain part of the transmitted

information symbols needs to be known to the receiver in order for this equalization operation to be possible. The estimated channel is then used to recover the received information symbols.

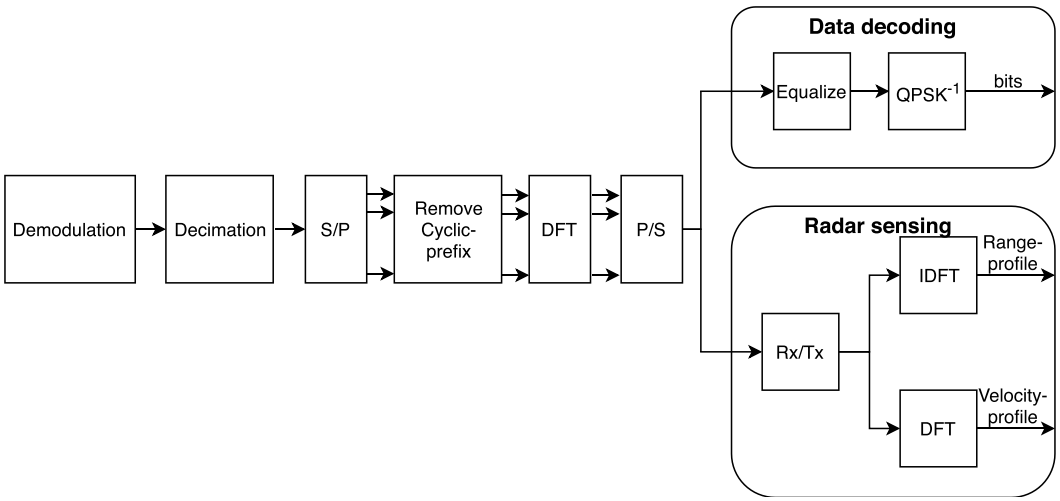

Figure 3.4: OFDM receiver.

In the radar sensing unit of the OFDM radar, the transmitted information is removed from the received information through an element wise division between the received I_{rx} and transmitted I_{tx} symbols prior to the channel equalization. Here it is assumed that the transmitted information is known to the receiver which is rarely an issue since the transmitter and receiver are often co-located in radar applications. The element wise division will result in a radar reception matrix I_{div} from which the range $r(k)$ and velocity $v(k)$ profile can be obtained using IFFT and FFT respectively. The process of obtaining the range profile is expressed below.

$$I_{div} = \frac{I_{rx}}{I_{tx}} \tag{3.4}$$

$$\begin{aligned} h(k) &= IFFT(I_{div}) = \tfrac{1}{N_{sub}} \textstyle\sum_{n=0}^{N_{sub}-1} I_{div}(n) \exp(j\tfrac{2\pi}{N_{sub}} nk) \\ &= \tfrac{1}{N_{sub}} \textstyle\sum_{n=0}^{N_{sub}-1} \exp(-j2\pi\Delta f \tfrac{2R}{c_0}) \exp(j\tfrac{2\pi}{N_{sub}} nk), \quad k = 0, ..., N_{sub} - 1 \end{aligned} \tag{3.5}$$

Observing (3.5), for a specific index k the two exponentials will cancel out which will result in a peak under the condition

$$k = \frac{2R\Delta f N_{sub}}{c_0}, \quad k = 0, ..., N_{sub} - 1 \tag{3.6}$$

where Δf is the subcarrier spacing, N_{sub} the number of subcarriers and R the range of the object.

3.2.3 MUSIC algorithm

MUltiple SIgnal Classification (MUSIC) is a type of super-resolution algorithm that has seen useful for estimating the angle of arrival in various radars [8]. The algo-

rithm has also seen some use for frequency estimation for example in FMCW radar [7].

In this thesis, the algorithm is applied to the OFDM radar in order to improve the range resolution and accuracy. Instead of retrieving the range profile by computing the IFFT of the quotient between the received I_{rx} and transmitted I_{tx} symbols like the conventional OFDM radar algorithm discussed in this thesis. The MUSIC algorithm takes a different approach by exploiting the eigenvalue decomposition of an auto-correlation matrix. The auto-correlation matrix is generated from a vector X that corresponds to one of the columns of the radar reception matrix I_{div}. Once the vector X has been retrieved, the $M * M$ sized auto-correlation matrix $R_{corrmat}$ can be generated as

$$R_{corrmat} = X * X^H \tag{3.7}$$

where the notation ^{H} indicates the Hermitian transpose. Notably, the length of vector X corresponds to the number of subcarriers N_{sub}. Hence, the size of the $M * M$ auto-correlation matrix needs to be less than or equal to the number of OFDM subcarriers, $M \leq N_{sub}$.

Further on, the eigenvalues of the auto-correlation matrix $R_{corrmat}$ are computed. The resulting p largest eigenvalues, where p is the expected number of exponential components, represent the signal subspace q_s, while the remaining $M - p$ elements represent the noise subspace q_n. Hence, by sorting the eigenvalues in a decreasing order the signal and noise subspace can be retrieved rather conveniently as the p first elements of the sorted sequence will represent the signal subspace while the remaining $M - p$ elements will represent the orthogonal noise subspace. The spectral peaks can then be found based on the noise subspace expressed in (3.8).

$$P_m(\omega) = \frac{1}{\sum_{i=1}^{M-p} |a(\omega)^H q_n|^2} \tag{3.8}$$

$$a(\omega) = [1, e^{j\omega}, e^{2j\omega}, ..., e^{(M-1)j\omega}]^T$$

where q_n is the noise subspace containing the last $M - p$ eigenvectors. The search vector $a(\omega)$ scans the noise subspace and will ideally project zero power if a specific element of the search vector contains a signal of interest. The inverse if this projection is then computed, resulting in peaks where minimal power is projected, estimating the radar range profile. Taking a closer look at (3.8) we note that the inner product $a(\omega)^H q_n$ amounts to an FFT of each q_n, thus (3.8) can be rewritten as

$$P_m(\omega) = \frac{1}{\sum_{i=1}^{M-p} |FFT(q_n)|^2} \tag{3.9}$$

The main drawback of the MUSIC algorithm is that the number of components (or targets) p needs to be known in advance which can limit the use of the algorithm. Additionally, it has a much higher computational complexity as compared to the conventional OFDM approach using IFFT described in section 3.2.2.

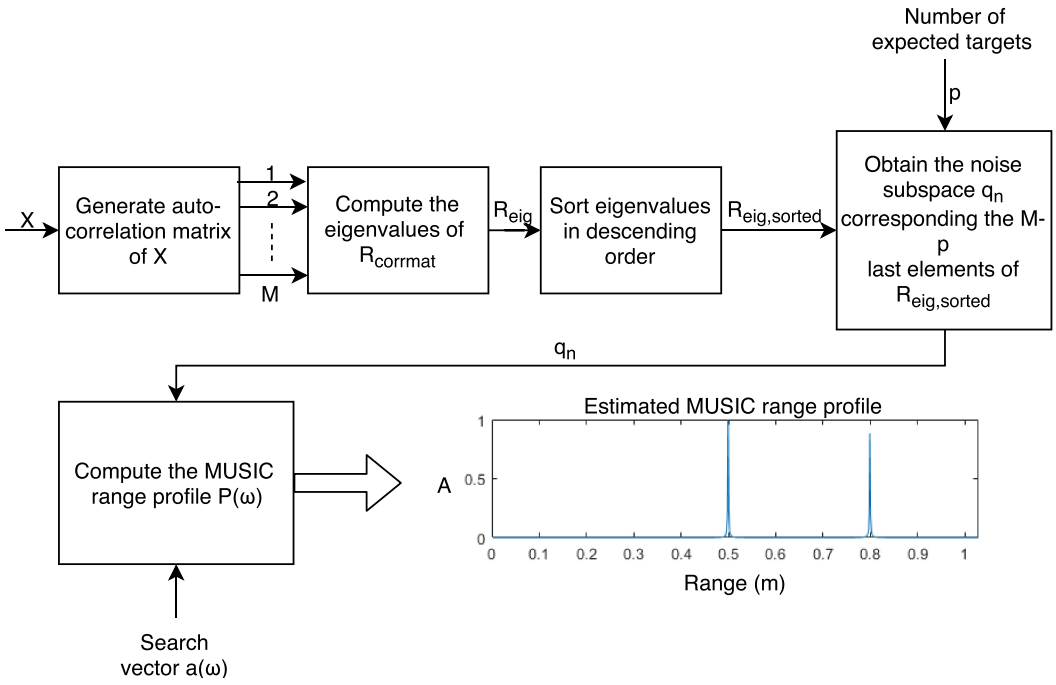

Figure 3.5: MUSIC algorithm flowchart.

4

Results and analysis

In this chapter, radar performance results from the OFDM and MSK-LFM waveform suggested in Chapter 3 are presented. Specifically, the range resolution of the two RadCom waveforms are initially evaluated through simulations. Furthermore, the radars and the corresponding simulation results are verified in a real-world environment using necessary hardware and radar equipment. In the final section of this chapter, the computational cost of the proposed radar sensing algorithms is evaluated.

4.1 Simulation and analysis of the MSK-LFM radar

This section presents and discusses simulation results from the MSK-LFM radar. In all simulations, the MSK-LFM waveform was generated according to section 3.1 with waveform parameters in Table 4.1.

Table 4.1: MSK-LFM radar simulation parameters.

Parameter	Value
Carrier frequency	80 GHz
Sampling frequency	16 GHz
Total bandwidth	1 GHz
Duration of signal	10 µs
Number of bits	128
Theoretical range resolution	15 cm

4.1.1 Evaluation of main and side-lobes of a single target

As mentioned earlier, range resolution is the radar's ability to distinguish targets that are close in range. A simple way to get a understanding how various radar waveforms perform in range resolution is to study their main-lobes. A narrow main lobe shows more promising range resolution. In an initial simulation, the MSK-LFM waveform was generated according to section 3.1 using waveform parameters in Table 4.1. The bandwidth is set to 1 GHz, which means that the system would need to be sampled at minimum 2 GHz to fulfill the Nyquist-Shannon criterion. However, if we would use a sampling rate of 2 GHz each sampling instance would be at a multiple of

$$R_s = \frac{c}{2f_s} = \frac{3e8}{2*2e9} = 7.5\,\text{cm}$$

This means that if the target is not located exactly at a multiple of R_s, unwanted range errors as big as 7.5 cm could occur as the range peak would be rounded to the nearest sampling instant. By oversampling the system these range errors can be reduced. Note that an increase in sampling rate does not necessarily increase the range resolution of the radar, rather it improves the accuracy. Taking a look at the simulation parameters in Table 4.1, the sampling frequency is set to 16 GHz which means that the max range error is $R_s = 0.9375$ cm for this simulation.

At the receiver side, the radar processing is done using the cross-correlation method described in section 3.1.2. In the simulation setup, a target is located at a distance of 3 m from the radar, which means that no range error will be introduced since the target is located at a multiple of $R_s = 0.9375$ cm. The results from this simulation is shown are Fig. 4.1. A sharp peak is detected at a distance of 3 m. The -3 dB width of the main-lobe is measured to $3.066 - 2.934 = 13.2$ cm and the side-lobe level to -13.24 dB. Judging from the main-lobe width of 13.2 cm, a range resolution of at least 13.2 cm should be expected.

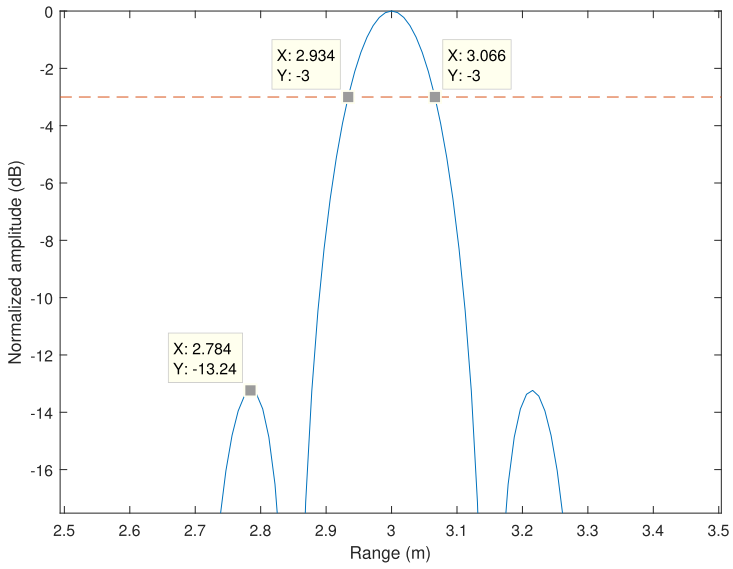

Figure 4.1: MSK-LFM radar range profile simulated using a single object placed at a distance of 3 m. Waveform parameters in Table 4.1 are used for this simulation. The red dashed line represent the -3 dB reference point.

4.1.2 Performance impact by varying the number of transmitted bits

The number of transmitted bits refers to how many bits that are sent during one pulse duration. To get an understanding of how the number of transmitted bits

impacts radar performance of the MSK-LFM waveform, the bit length has to be changed without changing other parameters of the signal. Hence, the number of samples per information bit has to be changed while keeping the same number of samples during one pulse duration. For instance, if the total pulse duration is made up of 8192 samples and we decide to transmit 128 bits, this means that $\frac{8192}{128} = 64$ samples will be used per information bit. If we then decide to transmit 1024 bits during one pulse duration, each bit will contain $\frac{8192}{1024} = 8$ samples. Hence, the number of transmitted bits has changed while keeping the total number of samples during one pulse duration the same.

For this simulation the information bits are generated randomly and the results are shown in Fig. 4.2. Notably, the side-lobes of the MSK-LFM signal are more suppressed when the number of transmitted bits is increased. In fact, the side-lobes are attenuated by -3.4 dB when increasing the number of transmitted bits from 128 to 4096 bits. On the other hand, the width of the main-lobe is barely affected by changing the bit length.

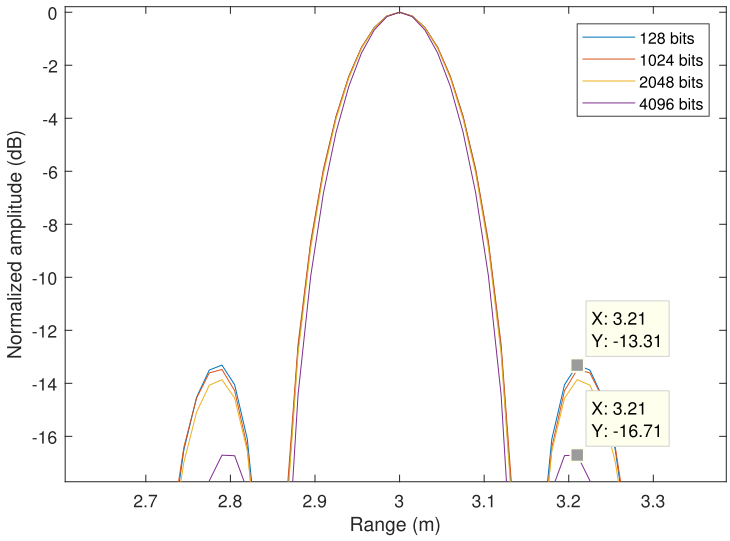

Figure 4.2: MSK-LFM radar range profile visualizing the bit length impact on the main and side-lobes from a single target scatter. Parameters in Table 4.1 are used for this simulation. The level of the side-lobes is reduced when increasing the the number of transmitted bits and the main-lobe width remains unaffected.

4.1.3 Multi-target setup

So far, simulations show that the MSK-LFM waveform has a -3 dB main-lobe width of 13.2 cm. Hence, the radar should at least be able to separate two targets at this distance from each other. A new simulation setup using the same parameters as before, Table 4.1, shows that two targets separated by 13.2 cm at 1 GHz bandwidth can still be seen as separate peaks, Fig. 4.3a. However, the targets are not appearing at their true range due to the side-lobes of nearby targets affecting the main-lobes.

As we saw from previous section, the level of the side-lobes can be attenuated by increasing the number of transmitted bits. By doing this, the side-lobes will not affect the main-lobes as much, causing the two targets to appear closer to their actual position seen in Fig. 4.3b.

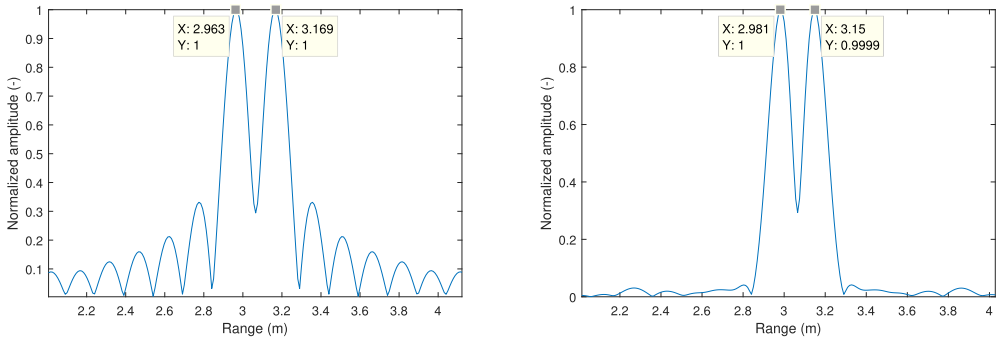

(a) 128 bits **(b)** 8192 bits

Figure 4.3: MSK-LFM radar range profile simulated using two objects placed at a distance of 3 m and 3.132 m. Waveform parameters in Table 4.1 are used for this simulation. The targets are clearly distinguishable but are not appearing at their true range because of side-lobe interference. However, by increasing the number of transmitted bits, seen in (b), the side-lobe level is reduced and the targets appear closer to their actual position.

4.2 Simulation and analysis of the OFDM radar

The OFDM radar is based on comparing the modulation symbols and performing IFFT to extract the range information unlike the MSK-LFM radar which is correlation based. For all OFDM simulations in this section, the OFDM waveform was generated according to section 3.2 with waveform parameters in Table 4.2.

Table 4.2: OFDM radar simulation parameters.

Parameter	Value
Carrier frequency	80 GHz
Sampling frequency	16 GHz
Up/Down sampling factor	16
Total bandwidth	1 GHz
Amount of subcarriers	128
Number of bits	128k
Cyclic prefix duration	3.2 µs
OFDM symbol duration	12.8 µs
Theoretical range resolution	15 cm

4.2.1 Increasing the FFT resolution

Since the OFDM waveform for the simulations is generated using 128 subcarriers, see Table 4.2, the size of the IFFT operation used for estimating the radar range profile is 128. This will give us 128 samples to display the range profile where each sample is placed 15 cm apart. Hence, the maximum range that the radar can see is $0.15 * 128 = 19.2\,\text{m}$ which is enough for the intended measurement setup. However, a sample every 15 cm will give us rather poor resolution and we will not get the true shape of the target main-lobe. To resolve this issue, the size of the IFFT operation can be increased by zero-padding the input signal to the IFFT unit with a certain factor. If the input is zero-padded by a factor of 10, a more exact shape of the actual range-peak will be displayed since we will have 10 times more samples: $128 * 10 = 1280$. Hence, instead of a sample appearing every 15 cm in the range profile, we will get a sample every $\frac{15\,\text{cm}}{10} = 1.5\,\text{cm}$ and the unambiguous range will still be at $0.015 * 1280 = 19.2\,\text{m}$.

The difference between not zero-padding and zero-padding the input by a factor of 10 is showcased by a OFDM simulation with two targets placed at a distance of 3 m and 3.15 m shown in Fig. 4.4. The two targets cannot be seen as separate peaks when using a IFFT size of 128, Fig 4.4a. Nonetheless, when the IFFT size is increased by a factor 10 the two targets are easily distinguishable with a certain offset caused by the side-lobes, Figure 4.4b.

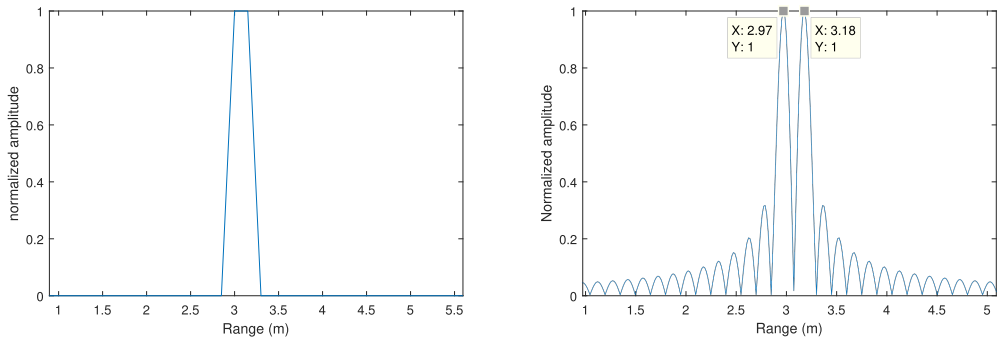

(a) **(b)**

Figure 4.4: OFDM radar range profile using different size IFFT with two targets placed at 3 m and 3.15 m. In (a) the IFFT size is 128, while in (b) the size is increased to 1280.

4.2.2 Evaluation of main and side-lobes of a single target

The purpose of this simulation is to measure the range resolution of the OFDM radar using the conventional Fourier based approach for radar sensing. For this simulation a single target scatterer is placed at a distance of 3 m, the input to the IFFT unit is zero-padded by a factor of 10 to get a more exact shape of the target's main-lobe. The resulting range profile is shown in Fig. 4.5. The -3 dB width of

the main-lobe is measured to 13.2 cm and the side-lobe level to -13.24 dB. Notably, these results are very similar to those obtained for the MSK-LFM radar in section 4.1.

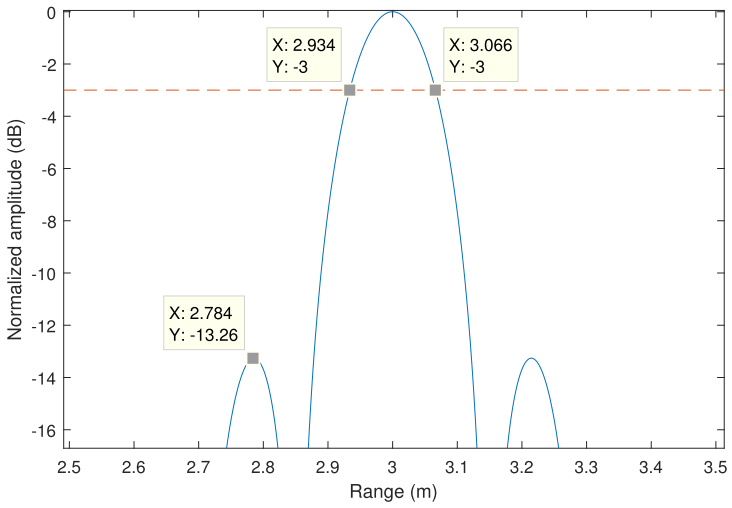

Figure 4.5: OFDM radar range profile of a single target placed at a distance of 3 m. Waveform parameters in Table 4.2 are used for this simulation. The red dashed line represent the -3 dB reference point.

4.2.3 MUSIC algorithm applied to the OFDM radar

Simulations from the previous section indicate that the traditional Fourier based OFDM radar has a range resolution of 13.2 cm at a bandwidth of 1 GHz. The most intuitive way to increase the range resolution would be to increase the bandwidth of the signal. However, it is good practice to be cautious with occupying large bandwidths. The MUSIC algorithm explained in section 3.2.3 is one way to increase the range resolution without affecting the bandwidth.

For this simulation, a comparison between the traditional Fourier and MUSIC based approach is made, using OFDM parameters in Table 4.2. The results in Fig. 4.12a indicate that two targets that are placed 10 cm apart are barely separable when using the Fourier based approach for radar sensing. However, when using the MUSIC algorithm, two clearly distinguishable peaks show up. In fact, when moving the targets as close to 6 cm apart, Fig. 4.12b, the MUSIC algorithm is still able to identify the two targets, while the Fourier based approach is only able to identify one target. This shows that the MUSIC algorithm is able to yield an improvement by at least a factor two compared to the Fourier based OFDM radar method. Notably, this is under ideal conditions whereas noise could possibly have an impact on the result which is addressed in section 4.2.5.

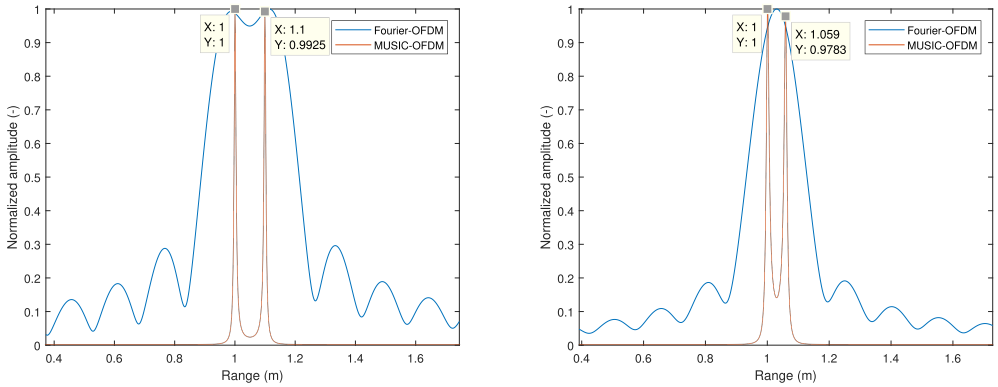

(a) Two targets at 1 m and 1.1 m. **(b)** Two targets at 1 m and 1.06 m.

Figure 4.6: Comparison between Fourier and MUSIC based OFDM radar at 1 GHz bandwidth. OFDM parameters in Table 4.2 are used for this simulation. For the MUSIC method, the size of the auto-correlation matrix is set to $m = 64$.

4.2.4 Size adjustment of MUSIC auto-correlation matrix

The size of the auto-correlation matrix used by the MUSIC algorithm, determines how many computations the MUSIC algorithms has to perform in order to compute the resulting range profile. On the other hand, the size of the matrix also determines the performance of the algorithm. Hence, there is a balance between performance and computational effort that has to be considered. Fig. 4.7 and the corresponding Table 4.3, shows simulation results of two targets placed at a distance of 1 m and 1.06 m using different sized correlation matrices. When the size of the auto-correlation matrix is increased, the two targets become more distinguishable which indicates that the range resolution is improved.

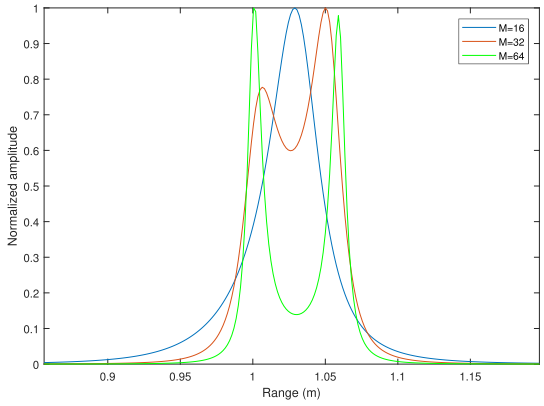

Figure 4.7: Range profile from MUSIC algorithm at 1 GHz bandwidth, using different sized "M" auto-correlation matrices. Two targets placed at a distance of 1 m and 1.06 m. OFDM parameters in Table 4.2 are used for this simulation.

Table 4.3: MUSIC algorithm, result of using different sized "M" auto-correlation matrices.

Estimated	**M = 16**	**M = 32**	**M = 64**
Target 1 (1 m)	1.029 m	1.007 m	1.0 m
Target 2 (1.06 m)	Not detected	1.05 m	1.059 m

4.2.5 SNR impact on MUSIC and Fourier approach

A noisy environment will most likely have a negative impact on radar performance. In a noise-free setup, the MUSIC algorithm outpreformed the Fourier approach in terms of range resolution and accuracy.

With additive white noise added to the OFDM signal, the two radar sensing methods were tested in a 2-target setup. Observing Fig. 4.8, the performance of the MUSIC algorithm seems to be easily affected by noise. At a SNR of -15 dB the MUSIC algorithm is barely able to distinguish two targets separated by 15 cm at a bandwidth of 1 GHz. However, by increasing the SNR to 5 dB the MUSIC algorithm shows very promising results. In the Fourier approach, Fig. 4.9, the SNR seems to have less impact on radar performance compared to the MUSIC method.

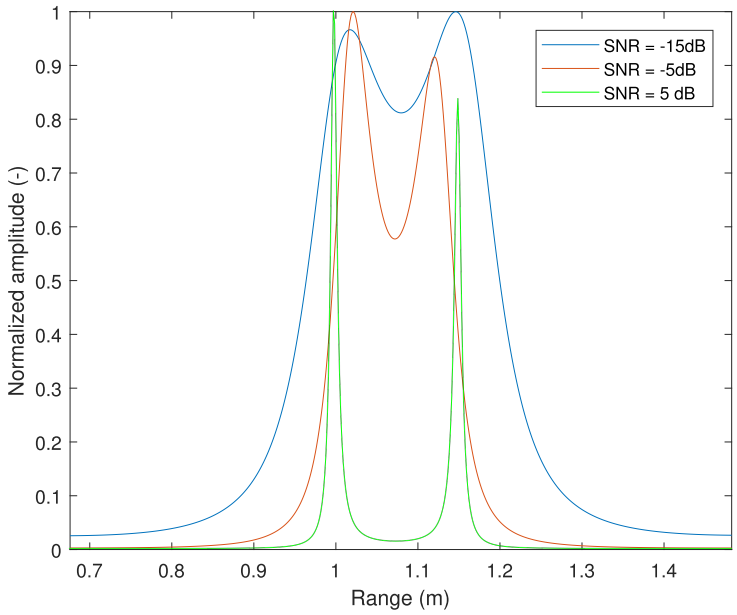

Figure 4.8: MUSIC algorithm SNR simulation. Two targets are separated by 15 cm at different SNRs using 1 GHz bandwidth. OFDM parameters in Table 4.2 are used and the size of the auto-correlation matrix is set to $M = 64$.

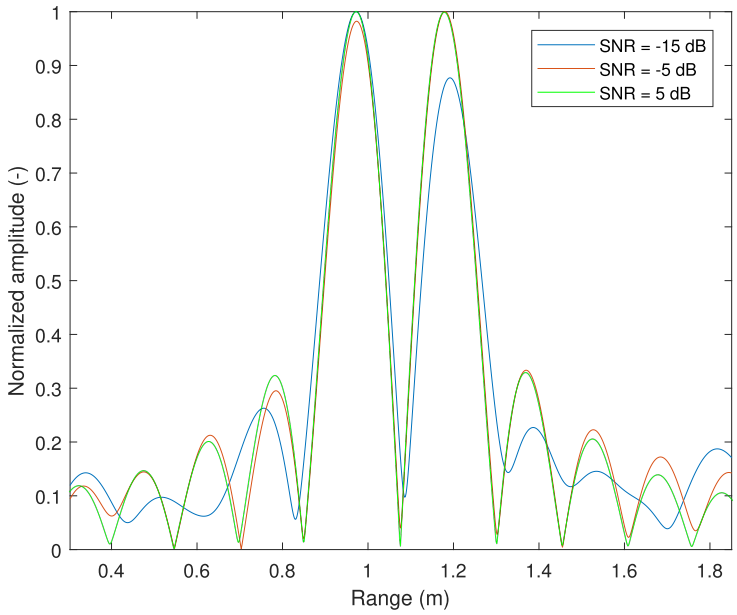

Figure 4.9: Traditional Fourier approach SNR simulation. Two targets are separated by 15 cm at different SNRs using 1 GHz bandwidth. OFDM parameters in Table 4.2 are used.

4.3 Overview of lab setup

On the transmitter side of the lab setup, a waveform is generated through MATLAB, in our case either the OFDM or MSK-LFM RadCom waveform is generated. At this stage the waveform is still at baseband and has a in-phase and quadrature-phase representation. The waveform is then sent to a 65 GSa/s Keysight M8195A AWG (Arbitrary Waveform Generator) which repeatedly outputs the uploaded waveform. The DAC output of the AWG is the I and Q signals of the waveform which are connected to a Gotmic E-band (80 GHz) transmitter which uses a 6 times on-chip mixer that is connected to a LO (Local Oscillator), making it possible for the signal to reach an RF of 80 GHz.

On the receiving side, a receiver from Gotmic is used which converts the signal back to baseband using a mixer associated with the same LO-signal as the transmitter side mixer. The resulting baseband signal is converted to a digital representation using a 240 GSa/s Teledyne Lecroy oscilloscope. The oscilloscope synchronizes on incoming data by triggering on a marker signal, which is a short pulse that is sent from the AWG every time the waveform is transmitted. The time between the marker signal and the reflected signal is the delay used for calculating the distance between the detected objects and the radar, visualized in Fig 4.10. Once the waveform is captured by the oscilloscope, the I and Q part of the signal is retrieved by MATLAB for post processing where the proposed radar sensing algorithms are applied.

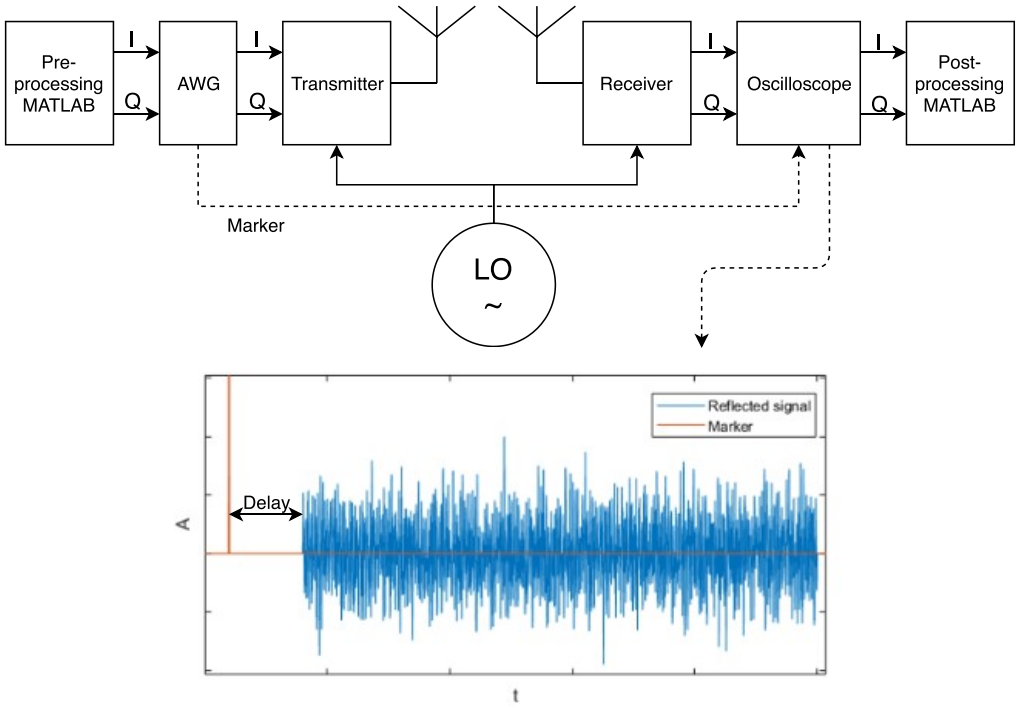

Figure 4.10: Block diagram of lab setup. The oscilloscope synchronizes on incoming data using a marker signal sent from the AWG.

Figure 4.11: Lab setup used by both the MSK-LFM and OFDM radar for measuring different kind of target setups. In this case a single metal pillar is placed roughly 1 m from the transceiver.

4.4 Measurement results of MSK-LFM radar

Waveform parameters used in the lab measurements for the MSK-LFM radar are shown in Table 4.4. In all lab setups the AWG was configured to operate at a sampling frequency of 16 GHz. The oscilloscope was set to a sampling frequency of 80 GHz which is a factor of 5 times larger than the AWG sampling frequency of 16 GHz. Hence, the retrieved signal from the oscilloscope was down-sampled by a factor 5 to get the ordinary sampling frequency of 16 GHz.

Table 4.4: MSK-LFM waveform parameters used for lab measurements.

Parameter	Value
Carrier frequency	80 GHz
Sampling frequency	16 GHz
Total bandwidth	1 GHz
Duration of signal	10 µs
Number of bits	128
Theoretical range resolution	15 cm

4.4.1 Single-target measurement

The purpose of this measurement is to verify the functionality of the radar in a real-world environment and obtain the range resolution by measuring the side-lobe levels and main-lobe width of a single target.

In this lab setup, a metal pillar with a diameter of 2 cm was placed roughly 1 m from the Tx/Rx antennas (located side-by-side), shown in Fig. 4.11. The range profile result from this setup is shown in Fig. 4.12 and a zoomed-in version of the range profile is shown in 4.12b, where the -3 dB width of the main-lobe is measured to $1.103\,\mathrm{m} - 0.9757\,\mathrm{m} = 12.73\,\mathrm{cm}$ and the side-level to -10.49 dB. In Table 4.7, a comparison between simulation and lab results is shown. Although the lab results showed a small decrease in main-lobe width, the side-lobe levels were a bit higher than simulations. Taking this into account, we should not expect a range resolution better than 13.2 cm at 1 GHz bandwidth, however this is still slightly better than the general range resolution of $\frac{c_0}{2*1e9} = 15\,\mathrm{cm}$.

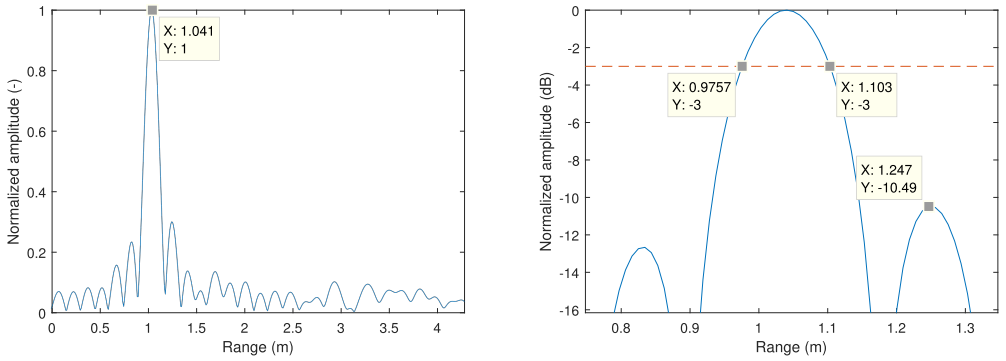

(a) **(b)**

Figure 4.12: Lab measurement of MSK-LFM radar using waveform parameters in Table 4.4. A metal pillar is located a distance of ruffly 1 m from the antennas. In (a) the range profile is displayed and in (b) a zoomed-in version of the same range profile is shown.

Table 4.5: Lab and simulation result comparison of MSK-LFM radar at 1 GHz bandwidth. The -3 dB main-lobe width and side-lobe level is compared

Environment	**-3 dB main-lobe width (cm)**	**Side-lobe level (dB)**
Simulation	13.2 cm	-13.24 dB
Lab	12.73 cm	-10.48 dB

4.4.2 Accuracy measurement

Accuracy is a measure on how well a radar can determine the true position of a object. The accuracy was obtained by first measuring a reference point of the target position, in this case a metal pillar. Once the reference point was obtained, the metal pillar was moved closer to the radar in a total of 5 steps of 3 cm. Referring to Table 4.4, the sampling frequency for this measurement is set to 16 GHz. Hence, the maximum accuracy error is $\frac{c}{2f_s} = \frac{c}{2*16e9} = 0.9375\,\text{cm}$ assuming that only one target is present. Additional close-by targets could possibly worsen the accuracy of the radar, as their side-lobes might affect the measured target's main-lobe position. However, in this setup only one target was present and the result is shown Fig. 4.13. The red dashed lines represent the theoretical maximum error which is $\pm$ 0.9375 cm. The measured data points are all within the error boundary and the largest error was measured to 0.75 cm.

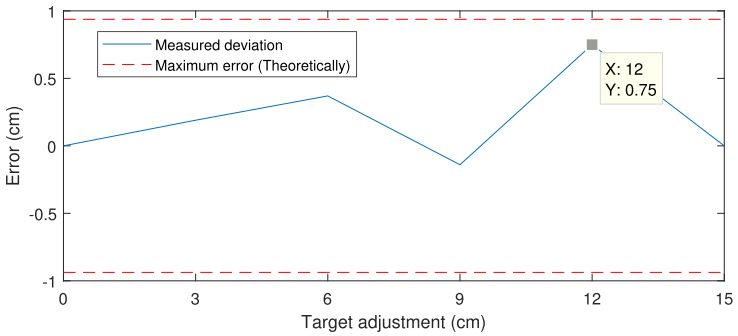

Figure 4.13: In-lab accuracy measurement of the MSK-LFM radar using waveform parameters in Table 4.7. A metal pillar is moved towards the transceiver in a total of 5 steps of 3 cm. All 5 measured points are within the error boundary of ± 0.9375 cm.

4.4.3 Multi-target measurement

From the initial lab measurement of the MSK-LFM radar, it was concluded that a range resolution of 13.2 cm can be achieved when using a bandwidth of 1 GHz. This is 12 % better than the general range resolution of $\frac{c}{2*1e9} = 15\,\text{cm}$. In the following lab setup, two metal pillars are placed 8 cm apart, which means that the radar will struggle to separate the two metal pillars when using a bandwidth of 1 GHz since the range resolution in that case will be 13.2 cm. By doubling the bandwidth to 2 GHz, the range resolution should be improved by a factor of two which should just be enough for the two targets to be distinguishable. Fig 4.14 shows both of these cases and evidently when using 2 GHz bandwidth, see Fig. 4.14a, the targets can be seen as two separate peaks with some skew caused by the side-lobes of the two targets. This indicates that the MSK-LFM radar works as intended and that an increase in bandwidth indeed improves the range resolution of the radar.

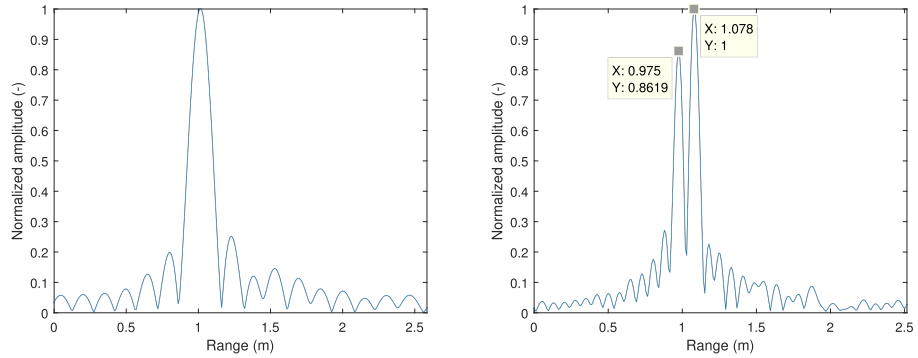

(a) **(b)**

Figure 4.14: Lab measurement of MSK-LFM radar using a two target setup where two metal pillars are placed 8 cm apart. Waveform parameters in Table 4.7 are used. The bandwidth is set to 1 GHz in (a) and 2 GHz in (b).

4.5 Measurement results of OFDM radar

Waveform parameters in Table 4.6 were used for all of the OFDM lab measurements. The sampling frequency of the AWG was set to 16 GHz and the oscilloscope's sampling rate to 80 GHz. The retrieved signal from the oscilloscope was down-sampled by a factor 5 to obtain the original sampling rate of 16 GHz.

Table 4.6: OFDM waveform parameters used for lab measurements.

Parameter	Value
Carrier frequency	80 GHz
Sampling frequency	16 GHz
Up/Down sampling factor	16
Total bandwidth	1 GHz
Number of subcarriers	128
Number of bits	128k
Cyclic prefix duration	3.2 µs
OFDM symbol duration	12.8 µs
Theoretical range resolution	15 cm

4.5.1 Single-target measurement using Fourier based approach

The purpose of this measurement is to verify the functionality of the OFDM radar in a real-world environment in addition to measure the main-lobe width and side-lobe levels of a single target.

For this lab setup, a OFDM waveform was generated with parameters in Table 4.6 and tested in a single target lab-setup using a 2 cm in diameter metal pillar placed roughly 1 m away from the Tx/Rx antennas. The Fourier based approach was used for radar sensing and the result is shown in Fig. 4.16. The main-lobe width was measured to $1.116\,\mathrm{m} - 0.9818\,\mathrm{m} = 13.42\,\mathrm{cm}$ which is slightly wider than what simulations showed. But on the other hand, the level of the side-lobes was measured to -14.19 dB which is ruffly 1 dB lower than what the simulation results showed. For a comparison between simulation and lab results, refer to Table 4.7. All things considered, the lab and simulation results are very similar, hence the range resolution of 13.2 cm, showcased by simulations, can also be expected in a real-world scenario.

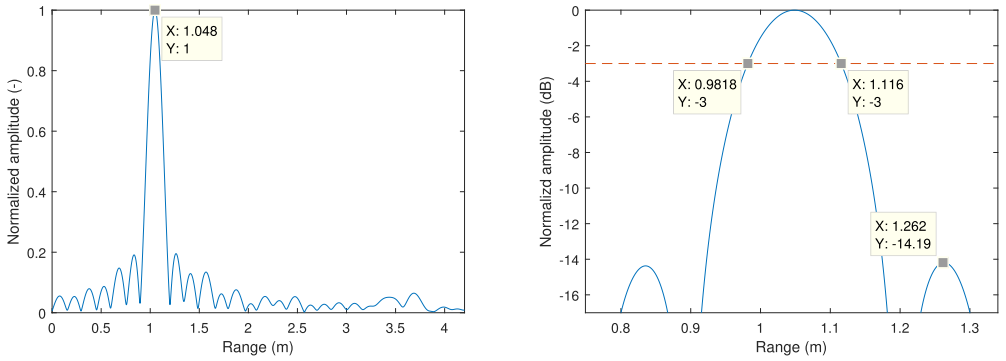

(a) **(b)**

Figure 4.15: Lab measurement of OFDM radar using waveform parameters in Table 4.6. A metal pillar is located a distance of ruffly 1 m. In (a) the range profile is displayed and in (b) a zoomed-in version of the same range profile is shown.

Table 4.7: Lab and simulation result comparison of Fourier based OFDM radar at 1 GHz bandwidth. The -3 dB main-lobe width and side-lobe level is compared

Environment	**-3 dB main-lobe width (cm)**	**Side-lobe level (dB)**
Simulation	13.2 cm	-13.24 dB
Lab	13.42 cm	-14.19 dB

4.5.2 Single- and multi-target measurement using MUSIC

For this measurement the MUSIC algorithm is used for radar sensing. Waveform parameters in Table 4.6 was used and the size of the auto-correlation matrix was set to $M = 64$.

As previously stated, a important aspect of the MUSIC algorithm is that the number of expected targets p needs to be known in advance. In the single target measurement setup, a metal pillar was placed ruffly 1 m from the antennas, in this case the number of expected targets was set to $p = 1$. The resulting range profile is shown in Fig 4.16a, a sharp peak is detected at 1.048 m which verifies that the MUSIC algorithm works for single target detection. However, the main purpose of the MUSIC algorithm is being able to identify multiple targets. Hence, in the next measurement two metal pillars were placed 30 cm apart. In this case the number of expected target was set to $p = 2$. The result is shown in Fig. 4.16b, the two targets are easily distinguishable.

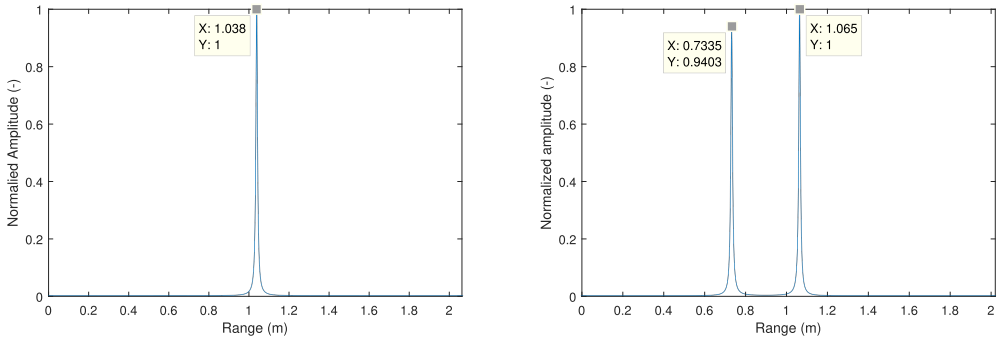

(a) **(b)**

Figure 4.16: Lab measurement of OFDM radar using the MUSIC approach for radar sensing. In (a) a single metal pillar is placed 1 m from the antennas whereas in (b) two metal pillars are placed 30 cm apart from each other.

4.6 Overview and computational cost

The cross-correlation algorithm for the MSK-LFM radar and the Fourier based algorithm for the OFDM radar yielded very similar results in terms of radar performance. In fact, both achieved a range resolution of 13.2 cm at a bandwidth of 1 GHz. The MUSIC algorithm for the OFDM radar, was able to improve the range resolution down to 6 cm. Although radar performance is of importance, it is not the only thing to consider when designing a radar system. As most radar applications require the radar to be able to operate in real-time under certain timing constraints, the computational complexity of the radar sensing algorithms is thus a very important aspect to consider.

Referring to the cross-correlation algorithm for the MSK-LFM radar described in section 3.1.2 it can be noted that two FFT operations are required to perform radar processing. Similarly, for the OFDM Fourier based radar algorithm, described in section 3.2.2, the most cost heavy computations are the two FFT operations that need to be computed. The MUSIC algorithm on the other hand, requires M FFT operations where M is the size of the auto-correlation matrix. Additionally, the computation of the MUSIC auto-correlation matrix and eigenvalue decomposition cannot be disregarded as these are also two cost heavy computations of the algorithm. Hence, the MUSIC algorithm is not an optimal solution when it comes to the computational complexity. To get a overview of the computational complexity of the radar sensing algorithms, the number of FFT operations each of the algorithms has to compute has been estimated. The corresponding number of complex multiplications is also given, assuming that the radix-2 FFT algorithm with complexity $O(n \log_2 n)$ is used [15]. The results are shown in Table 4.8. Note that the computational cost of the MUSIC auto-correlation matrix and eigenvalue decomposition is not included here, but by simply comparing the number of FFT computations of the algorithms it can be seen how high of a computational complexity the MUSIC

algorithm has.

Table 4.8: Comparison of the number of FFT operations each of the radar sensing algorithms has to compute. A rough estimate of the resulting number of complex multiplications is also given, assuming that each of the algorithms uses a 128 point FFT computed by the radix-2 FFT algorithm.

Radar sensing algorithm	**FFT operations**	**Complex multiplications**
MSK-LFM cross-correlation	2	$2 * (128 * \log_2(128)) = 1792$
OFDM-Fourier	2	$2 * (128 * \log_2(128)) = 1792$
OFDM-MUSIC(M = 64)	64	$64 * (128 * \log_2(128)) = 57344$

As can be seen in Table 4.8, the conventional MSK-LFM and OFDM radar sensing algorithm uses same number of resources for radar processing. However, including the fact that the systems are also intended for communication purposes, the OFDM system will be advantageous. The reason for this is that the OFDM radar algorithm operates on the received and transmitted OFDM symbols, thus, there are very few additional computations that has to be performed in order to retrieve the information bits. This is not the case for the MSK-LFM system as it requires two integration units, described in section 2.2.2, in the process of demodulating the communication symbols. Hence, for a complete RadCom system, the OFDM radar would be preferable choice as no additional computational heavy tasks has to be computed in order to demodulate the communication symbols.

5

Conclusion

In this thesis, a MSK-LFM and OFDM based radar waveform compatible with communication has been designed. Their corresponding radar sensing algorithms have been implemented and the performance of these have initially been presented through MATLAB simulations. The simulation results and the functionality of the waveforms have successfully been presented and verified in a real-life environment at a RF of 80 GHz.

For the MSK-LFM radar system, a cross-correlation method has been implemented and used for radar sensing. From simulations, a range resolution of 13.2 cm was achieved using a bandwidth of 1 GHz. This is an improvement by 12 % referring to the general range resolution of 15 cm at 1 GHz bandwidth. This result was also verified from lab measurements at a carrier frequency of 80 GHz. Additionally, it was found that the side-lobe amplitude levels can be reduced by increasing the number of modulated bits while keeping the same number of samples during one pulse duration.

In the OFDM case, a radar sensing algorithm merely operating on the transmitted and received modulation symbols has been implemented. Using this algorithm, the range resolution was measured to 13.2 cm at a bandwidth of 1 GHz. In the intent of improving the range resolution without increasing the bandwidth of the signal, a super-resolution algorithm known as MUSIC was implemented for the OFDM radar. Using the MUSIC algorithm, the range resolution of 13.2 cm was improved down to 6 cm, (45% improvement) while still using a bandwidth of 1 GHz. However, it was also discovered that the MUSIC algorithm is sensitive to noise and that the performance of the algorithm is greatly reduced at low SNRs, more so than the conventional OFDM radar sensing algorithm.

Furthermore, the computational cost of the radar sensing algorithms has been compared to each other. It was concluded that the MUSIC algorithm had a much higher complexity compared to the conventional OFDM and MSK-LFM radar sensing algorithms, which had very similar complexity. However, as the OFDM radar algorithm operate on the transmitted and received OFDM symbols, close to no additional computations had to be performed in order to retrieve the information bits. This was not the case for the MSK-LFM radar. Hence, for a complete RadCom system, where communication and radar sensing has to be performed simultaneously, the OFDM system would be preferred over the MSK-LFM system.

For future work, the communication aspect of the two RadCom systems can be evaluated more thoroughly by studying communication performance metrics such a bit-error rate (BER) at different SNRs, and investigate how radar performance is affected by communication performance and vice versa. Finally, further investigation of the MUSIC algorithm and its achievable range resolution in a real-life environment would be valuable for determining whether the algorithm is worth using considering its high complexity.

Bibliography

[1] W. Wiesbeck, L. Sit, M. Younis, T. Rommel, G. Krieger, A. Moreira, *"Radar 2020: The Future of Radar Systems"*, International Radar Conference, pp.188-191, Jul. 2015.

[2] C. Li, M. Tofighi, D. Schreurs, T. J. Horng, *"Principles and Applications of RF/Microwave in Healthcare and Biosensing"*, pp.208-219, Oct. 2016.

[3] X. Chen, X. Wang, S. Xu, J. Zhang, *"A Novel Radar Waveform Compatible with Communication"*, International Conference on Computational Problem-Solving, pp.177-181, Oct. 2011.

[4] C. Sturm, W. Wiesbeck, *"Waveform Design and Signal Processing Aspects for Fusion of Wireless Communications and Radar Sensing"*, Proc. IEEE, vol. 99, no. 07, pp.1236-1258, May 2011.

[5] J. Hasch, E. Topak, R. Schnabel, T. Zwick, R. Weigel, C. Waldschmidt, *"Millimeter-Wave Technology for Automotive Radar Sensors in the 77 GHz Frequency Band"*, IEEE Transactions on Microwave Theory and Techniques, pp.845-860, Mar. 2012.

[6] S. Schmidt, *"Multiple emitter location and signal parameter estimation"*, IEEE Transactions on Antennas and Propagation, vol. 34, no. 03, pp.276-280, Mar. 1986.

[7] M. A. Abou-Khousa, D. L. Simms, S. Kharkovsky, R. Zoughi, *"High-Resolution Short-Range Wideband FMCW Radar Measurements Based on MUSIC Algorithm"*, International Instrumentation and Measurement Technology Conference, pp.1-4, May. 2009.

[8] F. Belfiori, W. Rossum, P. Hoogeboom, *"Application of 2D MUSIC Algorithm to Range-Azimuth FMCW Radar Data"*, Proc. of the 9th European Radar Conference, pp.242-245, Feb. 2013.

[9] S. Pasupathy, *"Minimum Shift Keying: A Spectrally Efficient Modulation"*, IEEE Communications Magazine, vol. 17, no. 04, pp.14-21, Jul. 1979.

[10] D. Venu, N.V. Koteshwara Rao, *"A Cross-Correlation Approach to Determine Target Range in Passive Radar Using FM Broadcast Signals"*, International Radar Conference on Wireless Communications, Signal Processing and Networking, pp.524-529, Mar. 2016.

[11] L. Zhipeng, C. Xingbo, W. Xiaomo, S. Xu, F. Yuan, *"Communication Analysis of Integrated Waveform Based on LFM and MSK"*, IET International Radar Conference 2015, pp.1-5, Oct. 2015.

[12] R. Q. Huang, X. L. Zhao, Q. Zhang, J. Jia, *"Spectrum Extension Research of Radar-Communication Integrated Waveform"*, International Conference on Computer and Communications, pp.1804-1808, Oct. 2016.

[13] G. Hakobyan, M. Girma, X. Li, N. Tammireddy, B. Yang, *"Repeated Symbols OFDM-MIMO Radar at 24 GHz"*, Proc. IEEE, pp.249-252, Oct. 2016.

[14] C. D. Ozkaptan, E. Ekici, O. Altintas, C. H. Wang, *"OFDM Pilot-Based Radar for Joint Vehicular Communication and Radar System"*, IEEE Vehicular Networking Conference, pp.1-8, Dec. 2018.

[15] J. O. Smith, *"Mathematics of the Discrete Fourier Transform (DFT)"*, 2nd ed., W3K Publishing, pp.221-231, 2007.

[16] T. Hwang, C. Yang, G. Wu, S. Li, G. Li, *"OFDM and Its Wireless Applications: A Survey"*, IEEE Transactions on Vehicular Technology, vol. 58, no 4, pp.1673-1694, May. 2009.